High Power Laser Science and Engineering, (2014), Vol. 2, e27, 8 pages.

doi:10.1017/hpl.2014.29

Progress of the 10 J water-cooled Yb:YAG laser system in RCLF

Jian-Gang Zheng, Xin-Ying Jiang, Xiong-Wei Yan, Jun Zhang, Zhen-Guo Wang, Deng-Sheng Wu, Xiao-Lin Tian, Xiong-Jun Zhang, Ming-Zhong Li, Qi-Hua Zhu, Jing-Qin Su, Feng Jing, and Wan-Guo Zheng

Research Center of Laser Fusion (RCLF), CAEP, P.O. Box 919-988, Mianyang, Sichuan 621900, China

(Received 24 March 2014; revised 17 May 2014; accepted 14 June 2014)

Abstract

The high repetition rate 10 J/10 ns Yb:YAG laser system and its key techniques are reported. The amplifiers in this system have a multi-pass V-shape structure and the heat in the amplifiers is removed by means of laminar water flow. In the main amplifier, the laser is four-pass, and an approximately 8.5 J/1 Hz/10 ns output is achieved in the primary test. The far-field of the output beam is approximately 10 times the diffraction limit. Because of the higher levels of amplified spontaneous emission (ASE) in the main amplifier, the output energy is lower than expected. At the end we discuss some measures that can improve the properties of the laser system.

Keywords: Yb:YAG; V-shape amplifier; water-cooled; 10 J laser system

1. Introduction

It is becoming a reality that the energy crisis may be resolved by means of laser fusion, with significant on-going international research on inertial confinement fusion (ICF)[1] and the National Ignition Facility (NIF)[2, 3] coming closer to ignition. However, the laser driver of the NIF is based on Nd-doped glass[4, 5], which can operate only at low repetition rates (typically one shot every few hours)[6]. This kind of laser system cannot meet the requirements of inertial fusion energy (IFE). Therefore, it is necessary to develop a new type of laser driver for fusion that can work at a high repetition rate (typically 10–20 Hz)[7–11].

The following issues must be considered to obtain a high repetition rate for the IFE laser driver. Firstly, the laser system, especially the main amplifier system of the laser driver, must be actively thermal managed. Secondly, the gain medium of the amplifier must be able to operate at a high repetition rate – namely, when the laser system works repeatedly, the gain medium must dissipate heat to the outside to maintain itself in good order. Thirdly, the laser system must have a high energy conversion efficiency, so that electricity can be supplied from the power station.

Yb:YAG is an excellent gain medium for IFE laser systems[12–14] because of the long radiative lifetime of the upper energy level, which implies greater energy storage. Yb:YAG has a high thermal conductivity, thereby enabling the Yb:YAG laser system to operate repeatedly. The medium is free from several loss mechanisms (e.g. excited-state absorption, concentration quenching and upconversion) even at high dopant concentrations. In addition, Yb:YAG exhibits low quantum defects between the pump photons and the laser photons, which results in low thermal loading. The use of this material has increased following the emergence of Yb:YAG ceramics that meet the requirements of high energy in a single beam. Given these advantages, Yb:YAG (crystal or ceramics) may be widely used in laser systems with high repetition rates and high energy conversion efficiencies[15–22].

Unfortunately, Yb:YAG is a quasi-three-level system, and its properties are strongly affected by temperature[23, 24]. Hence, the thermal management for the amplifier must be carefully designed to avoid a high rise in temperature[25]. The thermal conduction, absorption and emission cross-section of Yb:YAG are high at low temperatures[26]. Low-temperature operation requires a large amount of additional energy, which reduces the overall energy conversion efficiency of the laser system. A low-temperature cooling setup also increases the complexity of the laser system.

Water is a raw material that exhibits a high thermal capacity and fluidity. As it is readily available and inexpensive, water is a suitable cooling medium for IFE laser drivers. The laser system, especially the main amplifier, must be properly designed to utilize water as a coolant.

Correspondence to: Zhen-Guo Wang, Mianshan Road No.64, Mianyang, Sichuan province, China, ZIP code: 621900. Email: zjg8861@163.com

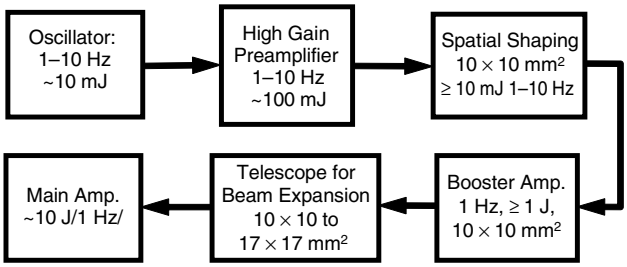

Figure 1. Structure of the proposed laser system.

In this paper, a room-temperature water-cooled 10 J Yb:YAG laser system is introduced. We present the structure of the laser system and describe the performance of its subsystem. Experimental results are discussed and solutions to increase the performance of the laser system are proposed.

2. Laser system design

2.1. Schematic of the laser system

The laser system (Figure 1) comprises a pulse generator, high-gain preamplifier, spatial shaping unit, booster amplifier, telescope for beam expansion, and main amplifier. The generator can produce laser pulses of approximately 10 mJ/10 ns, which are used as seed pulses for the laser system. The preamplifier provided an approximately 10 times gain and amplified the seed pulses to 100 mJ. The laser beam was expanded and clipped to a 10 mm × 10 mm square profile in the spatial shaping unit, reducing the energy of the laser pulse to approximately 10 mJ. The profile of the laser beam was configured to have a flat top, so that the beam could be properly amplified. The laser pulse was amplified to 1 J in the booster amplifier to achieve efficient energy conversion in the main amplifier. Finally, the main amplifier raised the energy of the laser pulses to approximately 10 J.

Figure 2 shows the layout of the laser system. To increase the efficiency of energy extraction, multi-pass amplification was used in the amplifiers. This process included non-image-relaying multi-pass V-shape amplification in the preamplifier, close-to-image-relaying multi-pass V-shape amplification in the booster amplifier, and image-relaying multi-pass V-shape amplification in the main amplifier. Image-relaying amplification enabled the uniform flat-top beam to be propagated to the gain medium for uniform amplification and avoided damage in the gain medium caused by near-field unevenness.

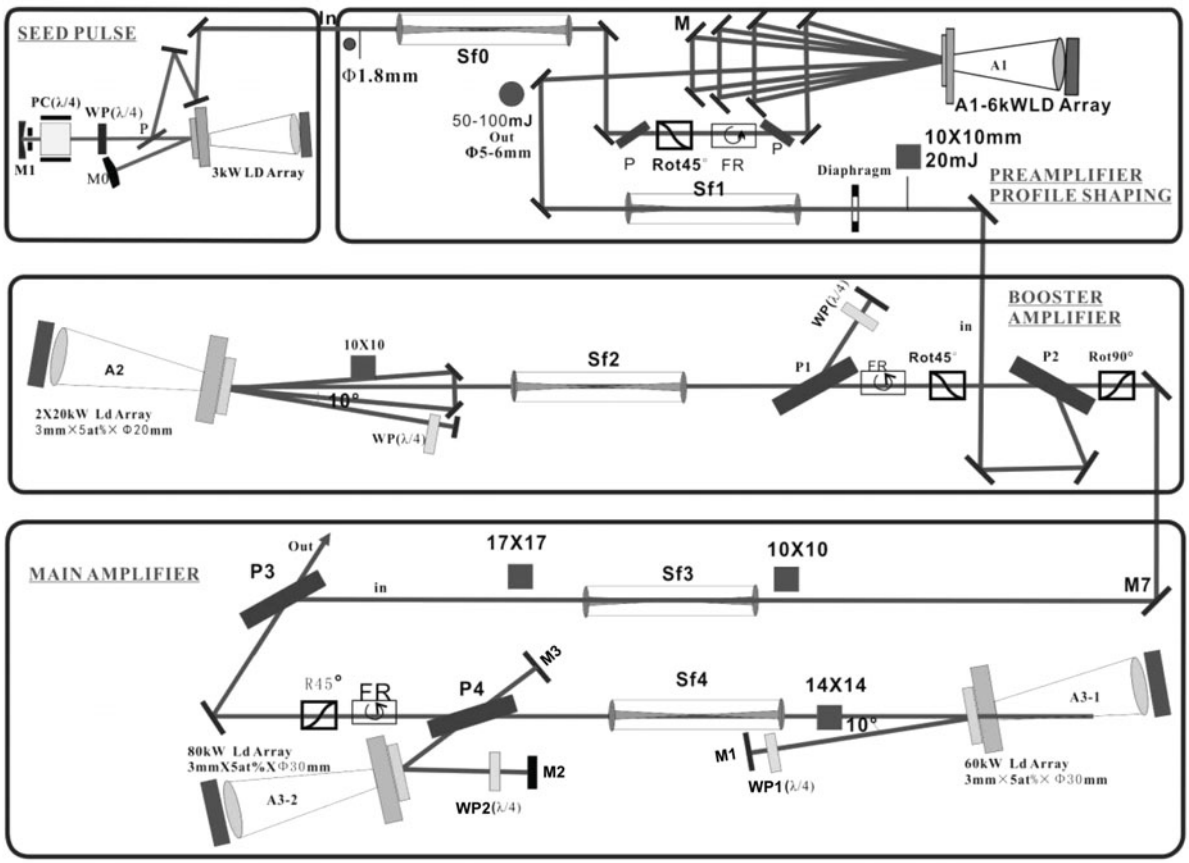

Figure 2. Layout of the laser system.

https://doi.org/10.1017/hpl.2014.29 Published online by Cambridge University Press

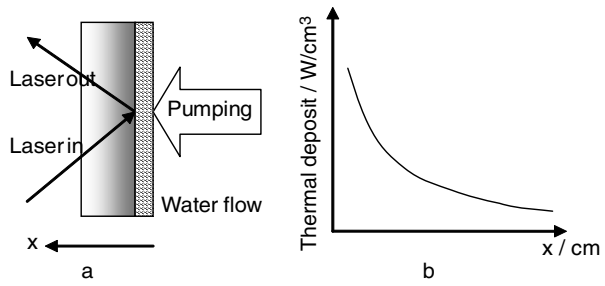

Figure 3. (a) Amplifier configuration and (b) thermal deposition in the gain medium as a function of x (in cm).

2.2. Configuration and thermal management of the amplifier

Figure 3(a) shows the amplifier configuration. The laser and pump light were located on opposite sides of the Yb:YAG crystal, with water flowing on the pump light side to cool the gain medium. Different dual-wavelength coatings were applied to the crystal: a coating that could reflect 1030 nm laser light and transmit 940 nm pump light was applied on the water-cooling side, while a coating that could transmit 1030 nm laser light and reflect 940 nm pump light was applied on the opposite side. This coating system ensured that the pump light and laser propagated through the crystal twice so that the pump light was adequately absorbed by the gain medium and the laser was amplified with high efficiency. The amplifier used was of the back-water-cooled type. One advantage of this type of amplifier lies in the ease of collection of water and cost efficiency; another advantage is the increase in thermal deposition on the pumping side (see Figure 3(b)). The amplifier configuration allows large amounts of heat to be extracted from the gain medium.

2.3. Pumping module for main amplifier

Laser diode (LD) arrays were used as a pumping source to improve the efficiency of energy conversion. The LD was modularized (Figure 4(a)) so that the diode could be produced in batches and easily used in large laser systems. In the 10 J laser system, the power of a single LD pump module is 10 kW (also called a 10 kW LD array). This system includes two planar arrays, each of which comprises about 24 bars; the power of the LD bar is about 200 W for a 200 A pump current. If the number of bars is less than 20 then the number of LD arrays and modules in the laser system increases and difficulties of system integration increase. The LD arrays were cooled by water flow through micro-channels. The LD bars were collimated by micro-lenses to ensure good propagation of the pump light.

High pump power densities are necessary for the Yb:YAG amplifier because some ion population is observed at lower lasing levels even at room temperature. An approximately 15–20 kW cm^{-2} power density is needed to achieve adequate energy storage in the gain medium. However, since

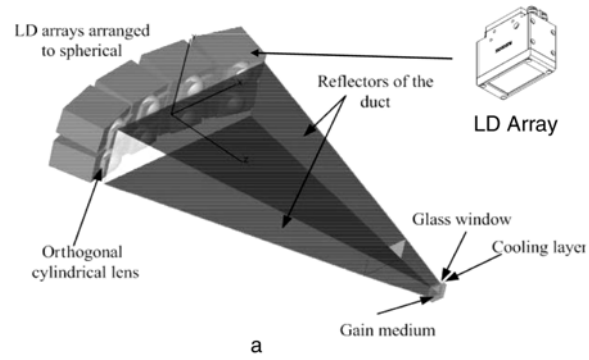

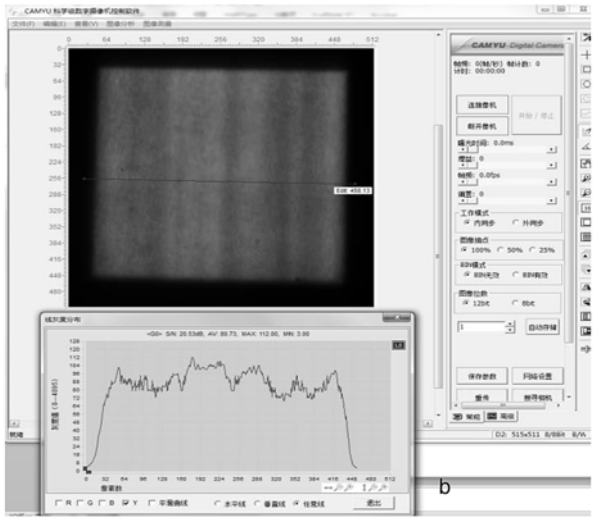

Figure 4. (a) Arrangement of LD modules with the duct and (b) output distribution.

the power density of the LD array is only 2–3 kW cm^{-2}, the requirements of a highly efficient laser amplifier cannot be met. Hence, the pump light must be focused and shaped to improve the power density and uniformity on the gain medium.

In our system, the LD arrays were arranged on a spherical segment (Figure 4(a)). The pump light was concentrated by lenses and ducts, which comprised two reflective plates covered with a silver coating. This LD array arrangement was selected to use planar LD arrays and test their properties. Moreover, in this arrangement, several planar LD arrays may be used, so the same optical components could focus the pump light emitted by the LD array. Finally, the reflection times of pump light on the ducts could be determined by this arrangement. In our pump module, over 23 kW cm^{-2} of pump power is achieved in a gain medium with an approximately 1.1 kW cm^{-2} LD array emission; the pumping efficiency reaches approximately 84%. Figure 4(b) shows the output of the pump module. The pumping is uniform. The maximum, minimum, and average values in the available area are approximately 111, 70, and 90, respectively, and the corresponding modulation in the

https://doi.org/10.1017/hpl.2014.29 Published online by Cambridge University Press

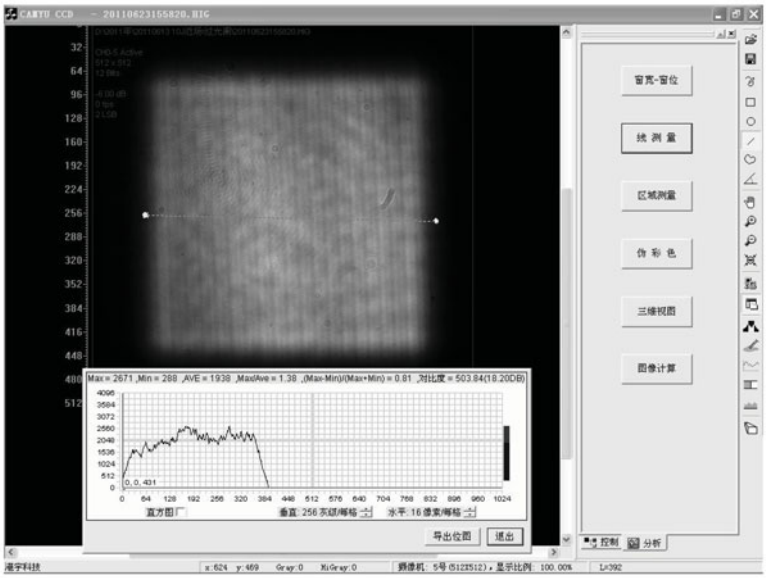

Figure 5. Laser beam near-field from the preamplifier.

available area is about 1.4:1. Pumping modulation may be attributed to the LD bars assembled in the LD arrays.

The total pumping power in the main amplifier was about 140 kW, resulting from fourteen 10 kW LD arrays; these LD arrays were arranged in two amplifier modules. One amplifier comprised eight 10 kW LD arrays, and the other comprised six 10 kW LD arrays.

3. Primary experimental results

The generator produces a 10 mJ/10 ns laser pulse with a Gaussian near-field and a wavelength of approximately 1030 nm. Moreover, the generator can work at 10 Hz. The seed pulse is eight-pass V-shape amplified to approximately 100 mJ in the preamplifier. At this stage, the beam is circular and exhibits a Gaussian profile, which is unfavourable for amplification; thus, the beam must be shaped into a square flat-top form. The beam energy must be at least 10 mJ so that enough energy can be obtained from the amplifiers. In our system, the laser energy is about 10 mJ after the shaping stage. The beam size is 10 mm × 10 mm, and ratio of the maximum and minimum modulation is about 1.38 (Figure 5), it basically meets the requirement of main amplifier.

The square flat-top beam is eight-pass V-shape amplified in the booster amplifier, after the booster amplifier, the fraction of maximum and minimum modulation is about 1.39 (Figure 6). The output energy of laser pulse is adjusted by controlling the pumping power. The maximum output energy reaches 1.2 J (Figure 7). The output energy of the beam is less than that of the initial design because of its small aperture and the low overlap between the laser beam and pumping area. However, for the 10 J laser system, a 1 J output energy is adequate for the subsequent amplification.

The laser energy results mainly from the main amplifier. We assessed the amplified spontaneous emission (ASE) in the main amplifier. The optimized product of concentration and thickness is about 15–20 at.% mm from the absorption efficiency. In our system, the doped ion concentration and thickness in the gain medium are 5 at.% and 3 mm, respectively. We evaluated the ASE using the spontaneous radiation signal from the amplifier. The top and bottom panels in Figure 8 show the spontaneous radiation signals from the 60 and 80 kW laser heads, respectively. The top panel (Figure 8) shows the spontaneous radiation signal increases rapidly until 600 μs; this increase in signal slows down thereafter, implying that energy storage increases within the duration of pumping. However, in the 80 kW laser head, the spontaneous radiation signal increases during pumping until 700 μs, then slows down, and remains constant thereafter. The energy storage fails to increase beyond 700 μs. Hence, the pump durations are set to 1 ms and 700 μs for the 60 and 80 kW laser heads, respectively.

A V-shaped multi-pass amplification was applied in the main amplifier (Figure 2) to improve the extraction efficiency of energy storage. A laser pulse was injected into the main amplifier through a polarizer (P4) and then passed through a spatial filter (SF4) to decrease the beam aperture from 17 mm × 17 mm to 14 mm × 14 mm. This pulse was subsequently double passed through the 60 kW laser head and V-shape amplified twice. In this section, the laser beam passed twice through the quarter-wave plate (WP1) and the direction of polarization was rotated by 90°. Hence, the laser pulse was reflected into the 80 kW laser head when it returned to the polarizer (P4). In the 80 kW amplifier, the laser was initially V-shape amplified twice, double passing through another quarter-wave plate (WP2);

https://doi.org/10.1017/hpl.2014.29 Published online by Cambridge University Press

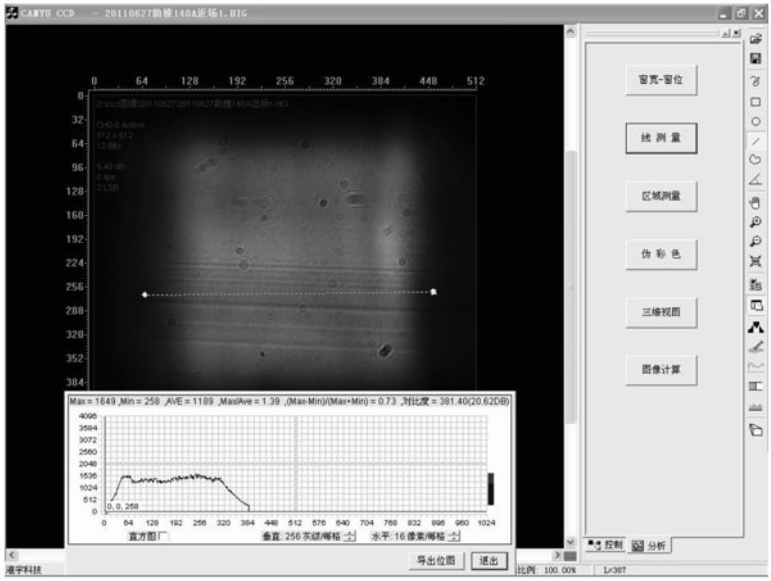

Figure 6. Laser beam near-field from the booster amplifier.

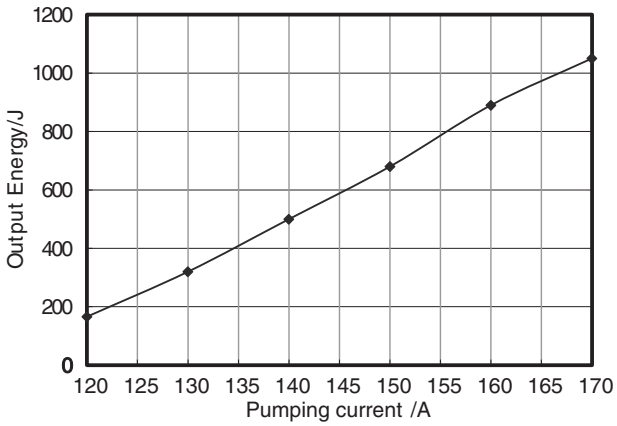

Figure 7. Output energy from the booster amplifier with different pumping currents.

its polarization was again rotated by 90°. When the laser pulse returned from the 80 kW laser head, it passed through the polarizer (P4), was directly reflected back by a mirror (M3), and then passed through the polarizer (P4) again back to the 80 kW laser head to perform a second series of double amplifications. Following the second series of amplifications the polarization of laser beam was rotated by 90° again. When the laser pulse returned from 80 kW laser head to the polarizer, it was reflected to the 60 kW laser head for yet another cycle of amplification. Following all the amplifications (four times each in the 80 and 60 kW amplifiers), the polarization of the laser beam was rotated 180°. From here, the laser pulse passed through the polarizer (P4) from the main amplifier, then through the Faraday rotator, and was exported from the laser system. The maximum energy obtained in the primary experiment is approximately 8.5 J (Figure 9); the near-field modulation is approximately 1.5 and the far-field is approximately 10 times the diffraction limit (Figure 10).

Near-field modulation is attributed to the pumping. Strip-shaped modulation is observed in the pumping output – in agreement with the arrangement of the LD bars. Hence, the best way to reduce modulation is to eliminate pumping modulation. The far-field of the system output is approximately 10 times the diffraction limit because of thermal aberrations in the gain medium. Even low thermal aberrations causes serious effects on the beam quality because of the small aperture of the pump area and the concentration of thermal deposition. Therefore, an enhanced procedure for thermal management must be considered; some techniques could include heating the edge of the gain medium and using adaptive mirrors.

4. Brief discussion of the experimental results

4.1. Output energy of the laser system

The output energy of the laser system in the integration experiment is less than expected in the initial design.

This result is attributed to the marked ASE in the amplifier, especially in the 80 kW laser head. The spontaneous radiation signal no longer increases after 700 μs pumping in this laser head, which implies that the ASE and parasitic oscillations increase; ASE especially decreases energy storage. Figure 11 shows the small signal gain (SSG) for different thicknesses of gain medium with the same product of concentration and thickness (15 at.% mm) under a 200 A pump current. The SSG improves markedly on

https://doi.org/10.1017/hpl.2014.29 Published online by Cambridge University Press

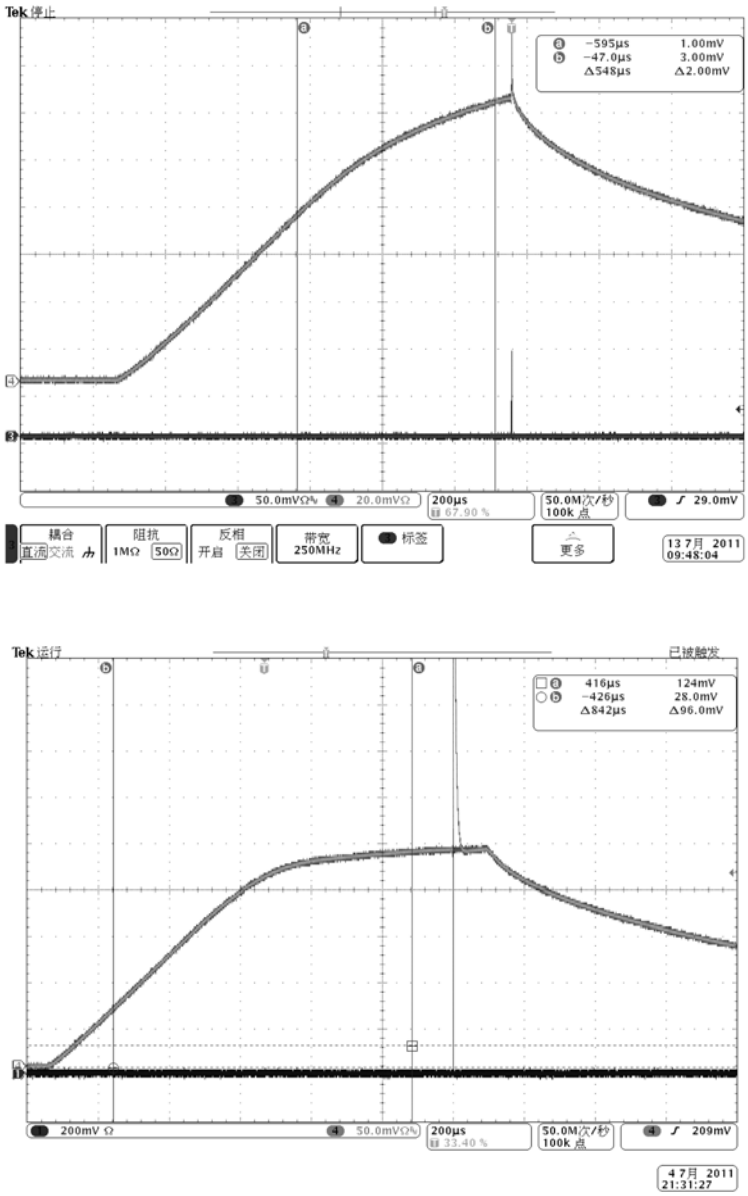

Figure 8. Amplifier fluorescence obtained at the heads with 60 kW (top) and 80 kW (bottom) pump powers.

increasing the medium thickness and decreasing the dopant concentration.

The low output energy may also be explained by the low overlap between the laser beam and the pumping area. A slight shift between the laser beam and active area may seriously affect this overlap because the apertures of the pump light and laser beam are small. Because the pump light exhibits a high angle of divergence in the proposed lens + duct LD pumping system, the active area increases with increasing distance from the incidence plane of the pump light, the laser exhibits good directivity, which results in low overlap. Hence, overlap must be considered during optimization of the concentration and thickness of the gain medium to yield high SSG.

The LD array comprises several LD bars – the directivity of these bars and the power uniformity of the LD arrays markedly affect the distribution of pump light on the gain medium. Figure 4 reveals that the profile of pump light on the gain medium exhibits modulation in the direction of the fast axes of the bars, which may cause modulation of the gain and energy storage in the amplifier. Similar modulation on the near-field of the output laser beam also results in damage to optical components. Hence, uniformity of the pump light must be improved to improve the output energy of the laser pulse.

The gain medium in our system is not surrounded by absorptive cladding, which could also absorb ASE from the gain area. Hence, the ASE light is reflected into the gain

https://doi.org/10.1017/hpl.2014.29 Published online by Cambridge University Press

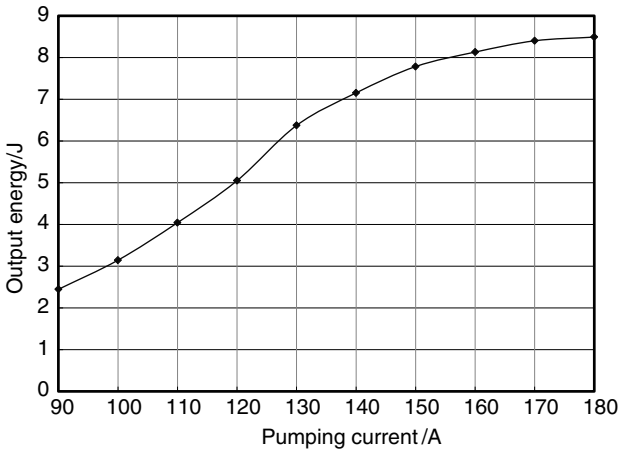

Figure 9. Output energy of the laser system at different currents.

area from the edge of the gain medium and energy storage in the amplifier is reduced. Even if the thickness of the gain medium is increased and the concentration of doped ions is decreased, re-amplification of the ASE cannot be eliminated. Therefore, the gain medium must be surrounded by absorptive cladding to avoid re-amplification of the ASE.

4.2. Effects of repetition rate

Thermal deposition and management differ respectively under various doping rates and thicknesses of the gain media. The laser performance of Yb:YAG crystal or ceramics is affected by temperature. Hence, we tested two types of Yb:YAG crystal with the same product of concentration and thickness (5 at.%@3 mm and 10 at.%@1.5 mm). The repetition rate ranges from 1 to 10 Hz and the pump current is 200 A. Figure 12 reveals that the SSG initially decreases with the repetition rate and then reaches an optimum value. This result is attributed to the low energy storage in the gain medium at the beginning of pumping – hence, the ASE and parasitic oscillations are low. A maximum SSG is observed with increasing pumping duration because of the effects of

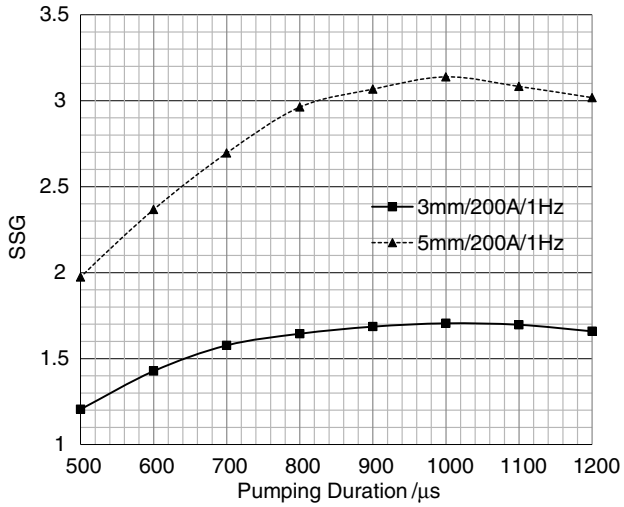

Figure 11. SSG at different pumping currents for 5 mm@3 at.% and 3 mm@5 at.%.

ASE, parasitic oscillations and temperature on the energy storage in the amplifier. In our system we set the repetition rate to 1 Hz during the primary integration.

5. Summary and conclusion

We have integrated a 10 J Yb:YAG laser system, in which the output energy of laser pulse is approximately 8.5 J under a 1 Hz repetition rate. The output energy of laser is slightly lower than that of the initial design because ASE and parasitic oscillations decrease the energy storage. Given the marked effects of temperature on the laser performance of Yb:YAG, the laser system works only at 1 Hz. For high repetition rates, the working point of the amplifier must be optimized. We aim to optimize the working point of the amplifier as well as the parameters of the gain medium in future research. During further development, we will heat the edge of the gain medium to balance the thermal aberrations in the pump area and clad the gain medium with an absorber to avoid re-amplification of the reflected ASE.

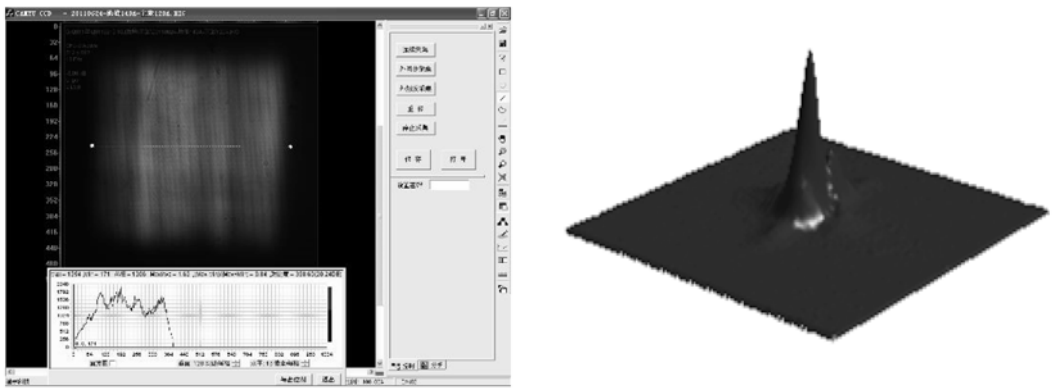

Figure 10. Near-field (left) and far-field (right) image of the laser beam.

https://doi.org/10.1017/hpl.2014.29 Published online by Cambridge University Press

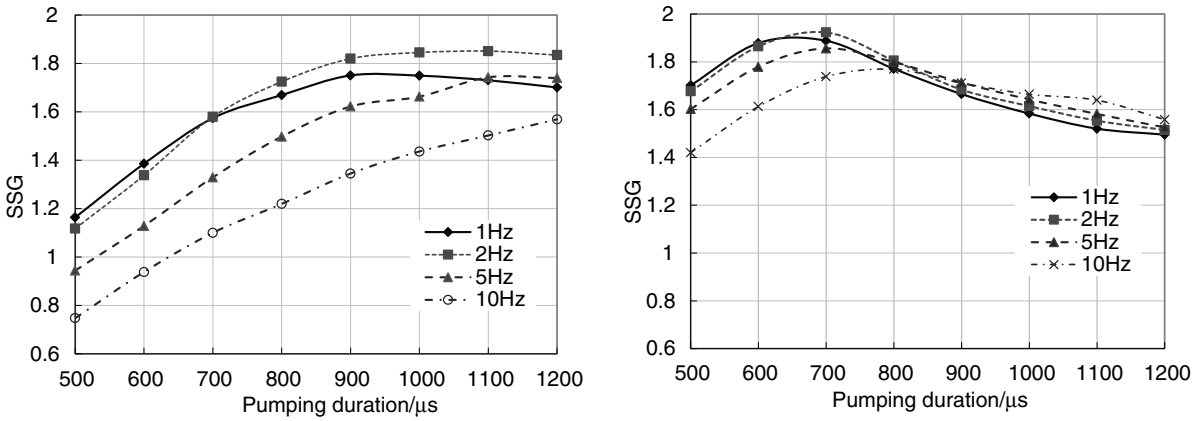

Figure 12. SSG in the amplifier with 5 at.%@3 mm (left) and 10 at.%@1.5 mm (right).

References

1. T. Land, *International Laser Operations Workshop, Livermore, CA, United States* (2013).
2. NIF closes in on alpha heating milestone (2014); Available from: http://fire.pppl.gov/#NewsSection.
3. O. A. Hurricane, D. A. Callahan, D. T. Casey, P. M. Celliers, C. Cerjan, E. L. Dewald, T. R. Dittrich, T. Döppner, D. E. Hinkel, L. F. Berzak Hopkins, J. L. Kline, S. Le Pape, T. Ma, A. G. MacPhee, J. L. Milovich, A. Pak, H.-S. Park, P. K. Patel, B. A. Remington, J. D. Salmonson, P. T. Springer, and R. Tommasini, Nature **506**, 343 (2014).
4. NIF Conceptual Design Team. National Ignition Facility Conceptual Design Report Volume 3: Conceptual (1994).
5. J. Horvath, UCRL-JC-124520 (1996).
6. N. Team, *National Ignition Facility User Guide* (2012).
7. C. Marshall, C. Bibeau, A. Bayramian, R. Beach, C. Ebbers, M. Emanuel, B. Freitas, S. Fulkerson, E. Honea, B. Krupke, J. Lawson, C. Orth, S. Payne, C. Petty, H. Powell, K. Schaffers, J. Skidmore, L. Smith, S. Sutton, and S. Telford, UCRL-JC-128084-REV-2 (1998).
8. M. Dunne, HiPER: a laser fusion facility for Europe (2007).
9. J. A. Caird, V. Agrawal, A. Bayramian, R. Beach, J. Britten, D. Chen, R. Cross, C. Ebbers, A. Erlandson, M. Feit, B. Freitas, C. Ghosh, C. Haefner, D. Homoelle, T. Ladran, J. Latkowski, W. Molander, J. Murray, S. Rubenchik, K. Schaffers, C. W. Siders, E. Stappaerts, S. Sutton, S. Telford, J. Trenholme, and C. P. J. Barty, in *Proceedings of 18th TOFE Conference* (2008).
10. F. Romanelli, Fusion Electricity A roadmap to the realisation of fusion energy, Specific Terms to prepare a technical roadmap to fusion electricity by 2050 (2012).
11. K. Yoshida, M. Yamanaka, M. Nakatsuka, T. Sasaki, and S. Nakai, Proc. SPIE **2966**, 2 (1997).
12. X. Wang, X. Xu, Z. Zhao, B. Jiang, J. Xu, G. Zhao, P. Deng, G. Bourdet, and J.-C. Chanteloup, Opt. Mater. **29**, 1662 (2007).
13. A. Bayramian, *7th International HEC-DPSSL Workshop 2012: Lake Tahoe, California* (2012).
14. S. M. A. A. C. Erlandson, A. J. Bayramian, A. L. Bullington, R. J. Beach, J. A. C. C. D. Boley, R. J. Deri, A. M. Dunne, D. L. Flowers, M. A. Henesian, E. I. M. K. R. Manes, S. I. Rana, K. I. Schaffers, M. L. Spaeth, C. J. Stolz, and S. J. Telford, Opt. Mater. Express **1**, 1341 (2011).
15. K. Ertel, S. Banerjee, P. D. Mason, P. J. Phillips, C. Hernandez-Gomez, and J. L. Collier, in *Proceedings of High Intensity Lasers and High Field Phenomena* (2012).
16. P. D. Mason, S. B. K. Ertel, P. J. Phillips, C. Hernandez-Gomez, and J. L. Collier, in *Proceedings of Advanced Solid-State Photonics* (2012).
17. W. Huang, J. Wang, X. Lu, and X. Li, Laser Phys. **23**, 035804 (2013).
18. D. Albach, M. Arzakantsyan, T. Novo, B. Vincent, and J.-C. Chanteloup, *7th International HEC-DPSSL Workshop 2012: Lake Tahoe, California* (2012).
19. P. D. Mason, K. Ertel, S. Banerjee, P. J. Phillips, C. Hernandez-Gomez, and J. L. Collier, in *Proceedings of CLEO 2012* CM3D.1 (2012).
20. I. B. Mukhin, O. V. Palashov, E. A. Khazanov, A. Ikesue, and Y. L. Aung, Opt. Express **13**, 5983 (2005).
21. J. Kawanaka, N. Miyanaga, T. Kawashima, K. Tsubakimoto, Y. Fujimoto, H. Kubomura, S. Matsuoka, T. Ikegawa, Y. Suzuki, N. Tsuchiya, T. Jitsuno, H. Furukawa, T. Kanabe, H. Fujita, K. Yoshida, H. Nakano, J. Nishimae, M. Nakatsuka, K. Ueda, and K. Tomabechi, J. Phys. Conf. Ser. **112**, 032058 (2008).
22. H. Yoshioka, S. Nakamura, T. Ogawa, and S. Wada, Opt. Express **17**, 8919 (2009).
23. J. Dong and P. Deng, J. Phys. Chem. Solids **64**, 1163 (2003).
24. A. Yoshida, S. Tokita, J. Kawanaka, T. Yanagitani, H. Yagi, F. Yamamura, and T. Kawashima, J. Phys. Conf. Ser. **112**, 032062 (2008).
25. C. Honninger, I. Johannsen, M. Moser, G. Zhang, A. Giesen, and U. Keller, Appl. Phys. B **65**, 423 (1997).
26. X. Li, X. Shi, P. Shi, M. Guo, G. Zhang, Y. Lu, and Q. Hu, Acta Opt. Sin. **21**, 1268 (2001).

https://doi.org/10.1017/hpl.2014.29 Published online by Cambridge University Press